

Connectivity of Turing structures

Teemu Leppänen¹, Mikko Karttunen¹, R.A. Barrio^{1,2}, and Kimmo Kaski¹

¹Laboratory of Computational Engineering, Helsinki University of Technology, P.O. Box 9203, FIN-02015 HUT, Finland

²Instituto de Física, Universidad Nacional Autónoma de México (UNAM), Apartado Postal 20-364 01000 México, D.F., México

(Dated: September 28, 2018)

It is well-known that in two dimensions Turing systems produce spots, stripes and labyrinthine patterns, and in three dimensions lamellar and spherical structures or their combinations are observed. We study transitions between these states in both two and three dimensions by first analytically deriving a control parameter and a scaling function for the number of clusters. Then, we apply large scale computer simulations to study the effect of nonlinearities on clustering, the appearance of topological defects and morphological changes in Turing structures. In the two-dimensional real space spotty structures we find some evidence of twin domain formation, of the kind seen in crystalline materials. With the help of reciprocal space analysis we find indication of other more general forms of order accommodation, i.e., eutactic local structures. Also a mechanism for the observed “connectivity transition” is proposed.

PACS numbers: PACS numbers: 82.40.Ck, 47.54.+r, 05.45.-a

I. INTRODUCTION

Nature presents a fascinating diversity of patterns in plants, animals and other natural formations arising often from complex physico-chemical processes [1]. Alan Turing was the first to show that a simple system of coupled reaction-diffusion equations for two chemicals could give rise to spatial patterns due to a mechanism called diffusion-driven instability [2]. These so-called Turing patterns have since been proposed to account for pattern formation in many biological systems, e.g. patterns on fish skin [3, 4], butterfly wings [5] and lady beetles [6] to mention a few. However, the first experimental evidence of a Turing structure was reported by Castets *et al.* [7], who observed a sustained standing nonequilibrium chemical pattern in a single-phase open reactor with chloride-iodide-malonic acid (CIMA) reaction. Currently, there is an increasing interest to develop simple and plausible mathematical models that could describe, at least qualitatively, these pattern formations [8, 9, 10, 11]. Although there is a variety of models that could potentially produce similar patterns, a Turing system is perhaps the simplest one.

The forms and variations of patterns generated by Turing systems have been studied by investigating the conditions for instability [12], assuming inhomogeneous diffusion coefficients [13], and by introducing domain curvature [14] and growth [15]. In addition, symmetries in Turing systems are of great interest, since they might have biological relevance, see e.g. Refs. [13, 16, 17]. Recently, we have studied the effect of dimensionality by simulating three-dimensional Turing systems, which displayed complex pattern formation [18]. While in two dimensions one obtains spots, stripes or labyrinthine patterns, in three dimensions complex shapes of, e.g. lamellae, spherical droplets and their combinations appear.

Previously, studies of Turing patterns have typically concentrated on reaction kinetic and stability aspects (see e.g. [19, 20]), while the issue of pattern structure and its connectivity has received less attention. Here, we focus on connectivity of Turing patterns and its dependence on the parameters of the system. We present a simple way to quantitatively characterize Turing structures and their connectivity. These meth-

ods are not only able to characterize the structures, but also to explain some of the effects of nonlinearities behind Turing patterns. We also demonstrate the existence of a “connectivity transition” when the nonlinear interactions of the Turing model are varied.

It was reported earlier that in generic 2D (3D) Turing models nonlinear cubic interactions favor stripes (lamellae) with both morphogens being connected through the system [4, 18]. On the other hand, quadratic interactions favor spots (spherical structures), in which case only one of the morphogens is connected. Thus, a connectivity transition appears when the nonlinear interactions are varied from being cubic to predominantly quadratic or vice versa. In order to characterize this transition between separated and connected structures, we define a dimensionless control parameter and a scaling function for the number of clusters. This is tested for a variety of system sizes and unstable modes. To characterize the resulting morphologies, we calculated the spatial Fourier spectrum to get the reciprocal space representation of the chemical concentrations and followed its evolution through the connectivity transition.

This paper is organized as follows. Next, we briefly describe the reaction-diffusion model of the Turing kind. Then, we discuss the concept of connectivity in these systems and the methods for characterizing the transition between different patterns. In Sec. IV, we present results of comprehensive numerical simulations, which is followed by Sec. V with a reciprocal space analysis. Then in Sec. VI we draw conclusions.

II. THE MODEL

A Turing system models the evolution of the concentrations of two chemicals, or morphogens, and is in general represented by the following reaction-diffusion equations

$$\begin{aligned} U_t &= D_U \nabla^2 U + f(U, V) \\ V_t &= D_V \nabla^2 V + g(U, V), \end{aligned} \quad (1)$$

where $U \equiv U(\vec{x}, t)$ and $V \equiv V(\vec{x}, t)$ are the morphogen concentrations, and D_U and D_V the corresponding diffusion co-

efficients setting the time scales for diffusion. The reaction kinetics is described by the two nonlinear functions f and g .

In this study we focus on the generic Turing model introduced by Barrio *et al.* [4], in which the reaction kinetics was developed by Taylor expanding the nonlinear functions around a stationary solution (U_c, V_c) . If terms above the third order are neglected, the system reads as follows

$$\begin{aligned} u_t &= D\delta\nabla^2 u + \alpha u(1 - r_1 v^2) + v(1 - r_2 u) \\ v_t &= \delta\nabla^2 v + v(\beta + \alpha r_1 uv) + u(\gamma + r_2 v), \end{aligned} \quad (2)$$

where $u = U - U_c$ and $v = V - V_c$ are the concentration fields. The parameters r_1 and r_2 set the amplitudes of the nonlinear cubic and quadratic terms, respectively, D is the ratio of the diffusion coefficients of the two chemicals, and δ acts as a scaling factor fixing the size of the system. Setting $D \neq 1$ is a necessary but not a sufficient condition for the diffusion-driven instability to occur. For details about the instability and the linear stability analysis of the model we refer the reader to Barrio *et al.* [4, 18].

From the linear stability analysis [4, 18] we obtain the dispersion relation and the conditions for the diffusion-driven instability as the region in k -space with positive growth rate, i.e., eigenmodes $u = u_0 e^{\lambda t}$ and $v = v_0 e^{\lambda t}$ with eigenvalues $\lambda(k) > 0$. In addition, one can analytically derive the modulus of the critical wave vector

$$k_c^2 = \frac{1}{\delta} \sqrt{\frac{\alpha(\beta + 1)}{D}}, \quad (3)$$

which was here determined for the case $\alpha = -\gamma$ (set to obtain only one stable state at $u = v = 0$ in the absence of diffusion). In a discretized three-dimensional cubic system, the wave number is of the form

$$|\vec{k}| = \frac{2\pi}{L} \sqrt{n_x^2 + n_y^2 + n_z^2}, \quad (4)$$

where L is the system size and n_x, n_y, n_z are the wave number indices (in a two-dimensional system $n_z = 0$). By adjusting the parameters and allowing only a few unstable modes, one can obtain several different parameter sets. As in our earlier work [18] we chose the parameters $D = 0.516$, $\alpha = -\gamma = 0.899$, $\beta = -0.91$ and $\delta = 2$ corresponding to a critical wave vector $k_c = 0.45$, and $D = 0.122$, $\alpha = 0.398$, $\beta = -0.4$ and $\delta = 2$ corresponding to $k_c = 0.84$.

In this study, we vary the parameters r_1 and r_2 in Eq. (2), since they control the appearance of stripes or spots. By gradually changing these parameters we observe a transition from spotty (2D) or spherical droplet (3D) patterns to striped (2D) or lamellar (3D) patterns. In order to investigate this transition, numerical simulations were carried out by discretizing the spatial dimensions into a square or cubic cell lattice and calculating the Laplacians in Eq. (2). In all of our simulations we used $dx = dy = dz = 1.0$. The equations of motion were iterated in time using the Euler scheme with time step $dt = 0.05$. The boundary conditions were chosen to be periodic, and initially both chemicals were distributed randomly over the whole system.

III. CONNECTIVITY

In the numerical simulations of Eq. (2) one deals with two concentration fields with characteristic wave lengths. In order to visualize this, the concentration of only one of the chemicals is typically plotted with a gray scale, since in this type of a system the fields are in anti-phase, i.e., if there is a large amount of chemical U in some sub-domain, the concentration of chemical V would be low there. These concentration fields vary continuously having diffuse boundaries. What do we mean by connectivity in patterns of chemicals?

To answer this question one can define sub-domains dominated by either chemical U or V , provided that the amplitudes of the patterns is large enough. If we define the boundary as the interface between sub-domains dominated by different chemicals, we can easily locate the boundaries, since the concentrations change rapidly, typically within one or two lattice sites. Now, if two points belong to the same domain, i.e., are not separated by a boundary, they are considered connected. The definition of the boundaries in this way is conceptual in the sense that in the U -dominated domains the concentration of V does not have to be zero, only much less than the concentration of U .

In Fig. 1 we show changes in the concentration fields, i.e., u and v , of a 2D system for different values of nonlinear parameters r_1 and r_2 in Eq. (2). When the cubic term (r_1) dominates, the resulting stationary pattern is striped with a small number of imperfections, see Fig. 1A. These imperfections can be considered as topological defects, or dislocations, which could serve as nucleation sites for spots. More dislocations appear (see Figs 1B-C) when the strength of the quadratic term is made larger. As the quadratic term increases, more spots nucleate and they arrange themselves to triangular structure and at the same time getting rid of the remaining stripes (see Figs. 1F-H). Finally when the cubic term is diminished even further, only spots remain. In this sequence of simulations the strength of the cubic term was changed relative to the quadratic term by using a single control parameter P , which we elaborate below. Nevertheless, the transition from striped to spotty pattern seems to happen quite abruptly in P . In the last frame of this sequence (Fig. 1I) we see a fully stabilized spotty pattern with almost perfect triangular symmetry in two different orientations such that there is a mirror plane or *twin boundary* between them.

Now, let us discuss patterns in Fig. 1 from the clustering point of view. In order to simplify this, and without loss of generality, we can assign zeros and ones to the whole lattice based on the chemical which dominates a given domain. With this mapping we can consider the number of clusters, which can be calculated using the well-known Hoshen-Kopelman algorithm [21] as in typical percolation problems. However, before applying this cluster algorithm let us first visually inspect possible shapes of extended clusters (Fig. 1). In Fig. 1A one can see that in the case of stripes the number of U - and V -dominated clusters is almost the same, and both types are extended dominantly in one of the dimensions. On the other hand, in the case of a spotty structure (Fig. 1I), chemical U appears as separate round clusters or spots, whereas chemical

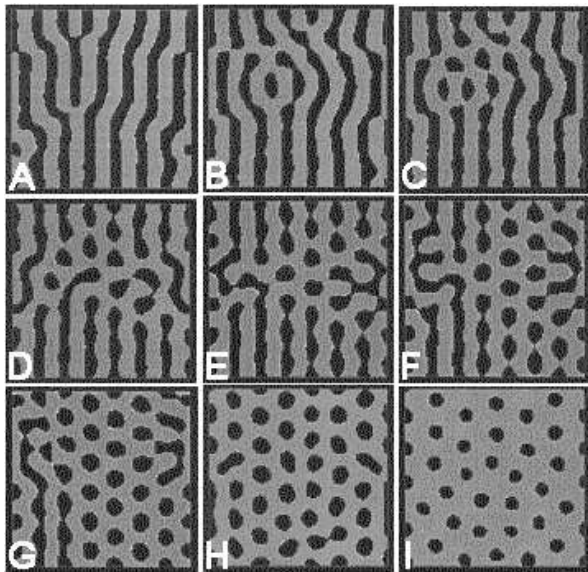


FIG. 1: Transition from stripes to spots. The patterns obtained after 50000 iterations in a 100×100 system with $k_c = 0.45$. Black corresponds to areas dominated by chemical U (zeros) and the lighter color chemical V (ones). Note that the difference in parameters between the figures is not constant: From A to I, $P = 22000, 120, 75, 65, 60, 55, 35, 15, 1$.

V forms only one connected cluster. Between these two limiting cases there is the transition region, depicted in Figs. 1D-F, where U -dominated clusters appear as spots and stripes in the form of a “string-of-pearls”. A question arises whether the transition from stripes to spots could be characterized in a reasonable way by the number of clusters? With the Hoshen-Kopelman algorithm we can directly determine the number of clusters (N) in the system, but we also need to define a single control parameter that N is a function of.

One should bear in mind that many different parameter pairs of nonlinear terms (r_1 and r_2) result in similar patterns. To obtain some general insight into the dynamics, we apply dimensional analysis [22] and derive a dimensionless control parameter for describing this behavior. The relevant dimensions are as follows

$$[\alpha] = \frac{1}{s}, \quad [r_1] = \frac{1}{[c]^2}, \quad [r_2] = \frac{1}{[c]s}, \quad (5)$$

where s denotes seconds and $[c]$ is an arbitrary unit of concentration. Thus, the control parameter P can be written in the following dimensionless form

$$P = r_1 \left(\frac{\alpha}{r_2} \right)^2. \quad (6)$$

The two limits of this parameter, i.e., $P \rightarrow \infty$ ($r_2 \rightarrow 0$) and $P \rightarrow 0$ ($r_1 \rightarrow 0$) yield stripes and spots (Figs 1A and 1I), respectively, as the two extremes in 2D. The same holds for 3D. Between these two limits a certain combination of striped (lamellar) and spotty (spherical droplet) patterns is expected to coexist (see Figs 1D- 1F).

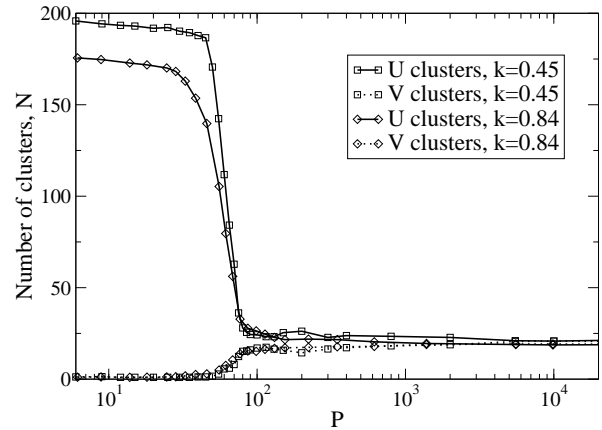


FIG. 2: The number of U (solid line) and V (dotted line) clusters as a function of the control parameter P . Diamonds: $k_c = 0.84$ in a 100×100 system, squares: $k_c = 0.45$ in a 200×200 system. In both cases the results were averaged over 20 simulations.

IV. SIMULATION RESULTS

In order to study the connectivity in two- and three-dimensional Turing patterns, we have performed extensive simulations using system sizes up to 5×10^5 lattice cells and up to 2×10^6 time steps to reach a stationary state. For all cases the results are taken as statistical averages of at least 20 separate runs. Using P (Eq. (6)) as a control parameter is plausible, since the transition from a striped (lamellar) pattern to a spotty (spherical droplet) pattern took place in a very narrow region of P regardless of the individual values of the nonlinear parameters (r_1 and r_2), the unstable mode (dictated by α and β) or the system size. This is clearly seen in Fig. 2, where the number of U - and V -dominated clusters is shown as a function of the control parameter P for two different cases in 2D. In our studies the P -space was scanned by keeping either r_1 or r_2 constant and by carrying out separate simulations for each value of P . From Fig. 2 it is clearly seen that the mode transition from spots to striped structure is quite sharp in P . The control parameter P serves the purpose of a unique transition variable, having a well-defined value for the transition to occur.

The most unstable mode for the smaller (100×100) system is with $k_c = 0.84$, while for the larger (200×200) system it is with $k_c = 0.45$. The larger system has smaller wave vector and thus the wave length, i.e., characteristic length of the pattern is larger. This is why the values on the vertical N -axis, are of the same order of magnitude. In order to compare the numbers of clusters one can normalize it by dividing with N_c^d , where $N_c = k_c L / 2\pi$, L denoting the linear system size (square or cube) and d the spatial dimension. N_c^d is the maximum number of spherically symmetric clusters in a d -dimensional system if the clusters were uniformly distributed and the effect of boundaries was neglected. Due to

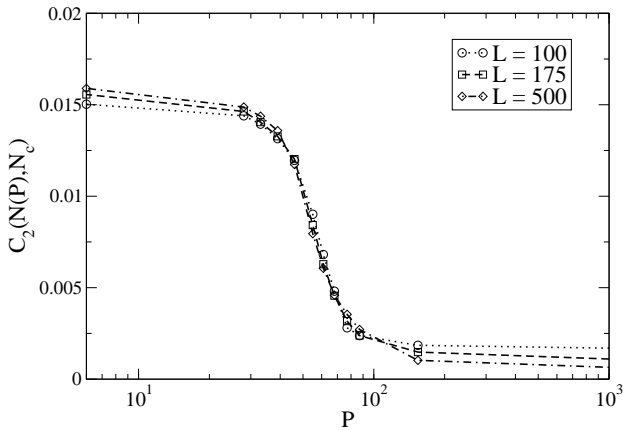


FIG. 3: The normalized number of U clusters as a function of P . System sizes are $L = 100$ (dotted), $L = 175$ (dashed) and $L = 500$ (dash-dotted).

the periodicity of the chemical structure, the number of clusters in the actual d -dimensional system can be estimated to be $N^d = (N_c + 1/2)^d$. However, an additional correction is required to take into account the effect of boundaries. One can estimate the number of additional partial clusters due to boundaries by estimating the length (area) of the boundary and the number of clusters within this domain (dN^{d-1}). As a result of this discussion we propose the normalization function for the number of clusters to be

$$C_d(N(P), N_c) = \frac{N(P)}{N_c^d} \left(1 - \frac{d}{N_c + \frac{1}{2}} \right), \quad (7)$$

where $N(P)$ is the calculated number of clusters for control parameter P . By revising the Hoshen-Kopelman algorithm one could have directly calculated the number of clusters by taking periodicity into account, in which case Eq. (7) reduces to $C_d(N(P), N_c) = N(P)/N_c^d$. However, this approach was not implemented and the normalization was carried out by using the Eq. (7).

We have also studied the effect of the system size on the mode transition in 2D. This is shown in Fig. 3, where the normalized quantity $C_2(N(P), N_c)$ is plotted for U -clusters against P for three different system sizes ($L = 100, 175$ and 500). Neglecting the number of V -clusters does not affect our conclusions, since the curves would be symmetrical as can be seen from Fig. 2. On the other hand, one can clearly see in Fig. 3 that the control parameter P succeeds in capturing the essential features of the transition. In addition, it can be seen that the normalization function of Eq. (7) scales the number of clusters such that it collapses onto the same curve with only very small deviations outside the transition.

If, on the other hand, one carries out the simulations for very small systems, finite-size effects can be observed. For small system sizes the $C_2(N(P), N_c)$ curve becomes very steep in the transition region. This would suggest that in the

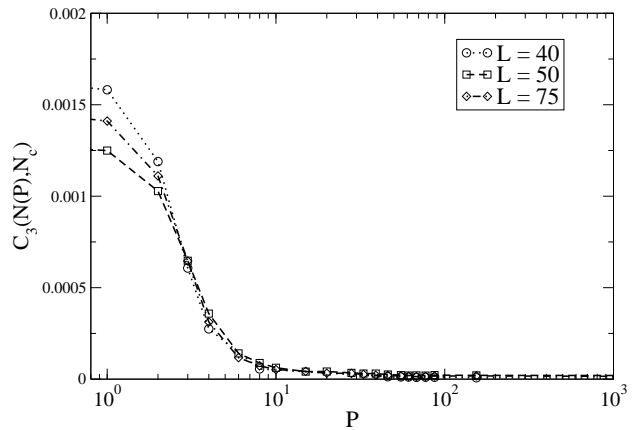


FIG. 4: The normalized number of U clusters as a function of P in a three-dimensional system. System sizes are $L = 40$ (dotted), $L = 50$ (dashed), and $L = 75$ (dash-dot).

limit of small systems, the transition would become almost discontinuous. However, the system cannot be made infinitely small since the (periodic) boundary conditions start to affect the behavior of the system. As discussed earlier the spots tend to nucleate from topological defects, or dislocations, of the striped pattern, i.e., from the points where the stripes coincide (Fig. 1). In the case of a small system even one dislocation can affect the morphology of the whole system and thus quickly transform stripes into a lattice of spots. In a larger system many dislocations have to appear at various sites to give rise to spots which in turn make the appearance of more spots favorable.

So far we have discussed our simulation results in 2D systems. We have also studied the connectivity transition extensively in three dimensions. In this case stripes and spots become lamellae and spherical droplets, respectively, and the structure seems more complicated especially in the transition region. For illustrations of three-dimensional Turing structures we refer the reader to Ref. [18]. In 3D the transition does not occur at the same point with respect to P as in 2D since the third dimension gives to the clustering process one more degree of freedom, and thus it is easier for the structures to connect.

This is indeed what one finds. Figure 4 depicts the normalized number of clusters for three different system sizes ($L = 40, 50$ and 75). One can see that the behavior of the system is different from two dimensions. Now, the transition occurs at a value of P which is a decade smaller than in 2D, since a smaller cubic nonlinear coefficient (r_1) favoring lamellar structures is sufficient for increasing connectivity in three-dimensional space. The significance of this large drop of the critical P -value remains unanswered. In addition, unlike in 2D we did not observe any finite-size effects for the smallest possible system sizes.

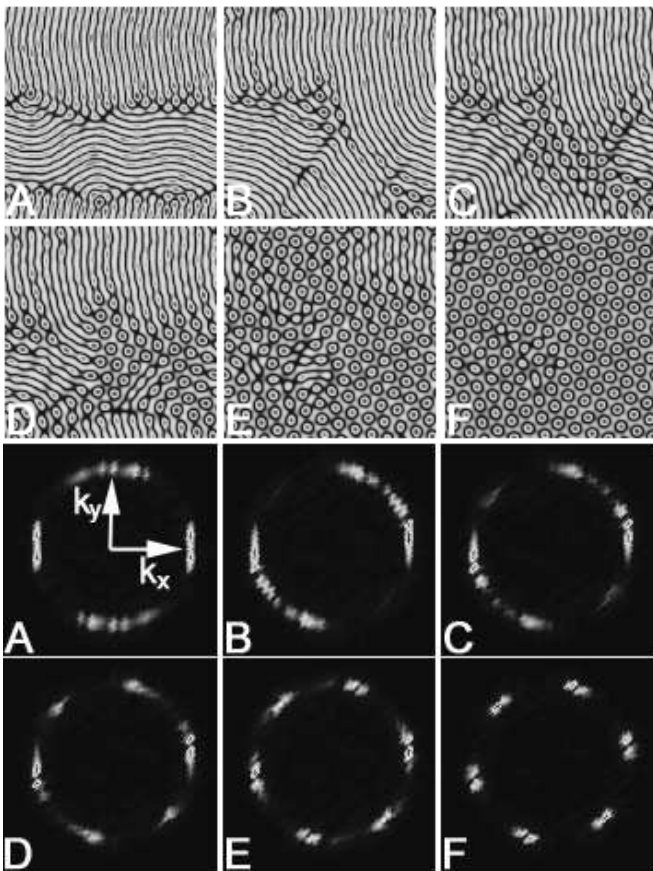


FIG. 5: Chemical concentration field $\hat{\rho}(\vec{r})$ in a system of size 200×200 (top) and the corresponding diffraction patterns in $k_x k_y$ -space (bottom) for $P = 22000, 150, 75, 70, 55, 12$. $(k_x, k_y) = (0, 0)$ is in the middle.

V. RECIPROCAL SPACE ANALYSIS

Next, we exploit another way to study the connectivity transition, namely the discrete Fourier transform of the concentration data in the wave vector space, \vec{k} , i.e.,

$$\hat{\rho}(\vec{k}) = \sum \rho(\vec{r}) e^{i\vec{k} \cdot \vec{r}}. \quad (8)$$

This approach has been used earlier, e.g. in connection of reaction-diffusion systems [23], Turing patterns [24], and to characterize the evolution of patterns [25]. The quantity $\hat{\rho}(\vec{k})$ corresponds to a diffraction pattern. Figure 5 shows a sequence of the original concentration fields and their diffraction patterns in a two-dimensional system for different control or transition field parameters, P .

In Fig. 5A, the diffraction intensity is predominantly to k_x -direction due to more stripes in y-direction, while the smaller diffraction intensity around the k_y -axis is due to the stripes in x-direction. The distance of these diffraction peaks from the origin gives the length of the wave vector of the unstable mode, while its width in the perpendicular direction describes deviations of stripes from the principal directions due to stripe tilting and bending. In Fig. 5B the diffraction intensity be-

comes more spread around the (k_x, k_y) diagonal, as a result of appearing dislocations and nucleating spots. After that in Figs. 5C-D the diffraction intensity starts splitting into separate peaks due to more spots forming, then developing into six separate equidistant (from the origin and from each other) intensity peaks as evident in Figs. 5E-F. This hexagonal symmetry in the reciprocal space is because the system evolves towards regular spotty pattern with predominantly triangular symmetry in the real space. However, these diffraction peaks are somewhat spread and in fact each peak split in two, which indicates that the triangular symmetry is not perfect over the whole system.

If one examines the real space picture of spots in Fig. 5F, one might think that there are fairly large disordered regions that deviate from the ideal triangular perfect lattice of spots. However, the corresponding reciprocal space picture reveals that this is not so, since it does not show diffuse diffraction pattern or a ring due to orientational disorder, but it does show a double peak structure as can be seen in crystalline materials due to twinning or low-angle grain boundaries. The existence of this kind of boundaries is common place in any nucleation mechanism and usually it is associated to the fact that twinning or low-angle grain boundaries require only small local displacements at low energy cost. In the present case, however, there is no energetics involved and in Fig. 5F it is difficult to find clear twinning, which we found in Fig. 1I. There are other more general ways of establishing order, namely the appearance of *eutactic* local structures defined in the study of regular polytopes [27]. It has been recently proposed [28] that eutacticity is a very important property exhibited not only by crystalline and quasicrystalline lattices, but also by the geometrical forms of some biological systems. The presence of order in these Turing patterns, as revealed by their clear diffraction patterns, suggests that the principles governing the preference for eutactic structures also apply to the present case.

Here, we have done the reciprocal space analysis for 2D systems, but the same analysis can easily be extended to 3D systems by fixing the orientation of one of the spatial vectors, thus obtaining an in-plane diffraction graph. These diffraction patterns, however, are expected to look more or less the same as in 2D, which can be understood on the basis that almost every cross-section of a lamellae or spherical droplet pattern in 3D would look as striped or spotty pattern, respectively.

VI. DISCUSSION

In this study, we have investigated the connectivity of spatial patterns generated by the reaction-diffusion mechanism both in 2D and 3D. This was done by cluster analysis for the dominating chemical. Since several different combinations of parameters in a Turing system can produce similar patterns, we derived a dimensionless control parameter to investigate the effects of nonlinearities. The numerical simulations were consistent with the predictions drawn from the dimensional analysis, and the system showed a transition in the proximity of the same P -value irrespective of the individual system

parameters. With help of an analytically derived normalization function, the number of clusters collapsed onto the same master curve independently of the system size or the unstable mode.

From biological perspective, the characteristics of the Turing system presented here could be important. The fact that the transition from striped or lamellar to spotty or spherical droplet structures does not depend on the size of the system or the specific parameters involved, but just the combination of the nonlinearities (P), makes the mechanism very general. In addition, the observation that irregular structures are not as stable as regular structures could be used to explain the steepness of the transition: Unfavorable structures corresponding to the transition domain occupy minimal volume of the phase space (possible structures).

The presence of eutacticity is well known in atomic crystal structures. The fact that similar geometric principles seem to be acting also in the formation of Turing patterns could be an important feature in favor of their application in the study of the geometrical forms of some simple living organisms. This could also support the idea that Nature prefers geometrical forms generated from eutactic stars [28]. This very simple analysis of Turing patterns and their morphological transitions due to nonlinearities could open up a new way of investigating universal features of patterns obtained by very different mechanisms.

The approach we have taken here to study pattern formation shares common features with percolation and could be studied to certain extent as such. Percolation of morphogens

to different directions is not as interesting a measure as the number of clusters, since it holds only a binary value and does not capture features of the morphological structure effectively. However, if one considers the field of biological applications, where Turing systems are often used, percolation behavior is interesting and has been used for studying some biological problems [29].

If one considers the patterns in Fig. 1 one can observe that in the first frame both morphogens have percolated in the vertical direction. On the other side of the transition one of the morphogens has not percolated while the other has done so in both directions. Should one of the chemicals be favorable for diffusion, these two opposite stages obtained by a small variation of nonlinear parameters could for example correspond to chemical concentrations in tissue as signaling via diffusion is either enabled or disabled. However, one should always be careful in making suggestions for biological applications due to complexities of nature not yet understood.

Acknowledgments

We wish to thank János Kertész for helpful discussions, and one of us (R. A. B.) wishes to thank the Laboratory of Computational Engineering at Helsinki University of Technology for its hospitality. This work has been supported by the Academy of Finland through its Centre of Excellence Program (T. L. and K. K.).

-
- [1] P. Ball, *The self-made tapestry: pattern formation in nature* (Oxford Univ. Press, Oxford, 2001).
 - [2] A. M. Turing, Phil. Trans. R. Soc. Lond. **B237**, 37 (1952).
 - [3] S. Kondo and R. Asai, Nature **376**, 678 (1995).
 - [4] R. Barrio, C. Varea, J. L. Aragón, and P. Maini, Bull. Math. Biol. **61**, 483 (1999).
 - [5] T. Sekimura, A. Madzvamuse, A. J. Wathen, and P. Maini, Proc. Roy. Soc. London B **267**, 851 (2000).
 - [6] S. S. Liaw, C. C. Yang, R. T. Liu, and J. T. Hong, Phys. Rev. E **64**, 041909 (2002).
 - [7] V. Castets, E. Dulos, J. Boissonade, and P. De Kepper, Phys. Rev. Lett. **64**, 2953 (1990).
 - [8] G. Nicolis and I. Prigogine, *Self-Organisation in Non-Equilibrium Chemical Systems* (Wiley, New York, 1977).
 - [9] H. Haken, *Synergetics, An Introduction* (Springer-Verlag, Berlin, 1977).
 - [10] H. Meinhardt, *Models of Biological Pattern Formation* (Academic, New York, 1982).
 - [11] J. D. Murray, *Mathematical Biology* (Springer Verlag, Berlin, 1993).
 - [12] L. Szili and J. Toth, Phys. Rev. E **48**, 183 (1993).
 - [13] R. A. Barrio, J. L. Aragón, M. Torres, and P. K. Maini, Physica D **168-169**, 61 (2002).
 - [14] C. Varea, J. L. Aragón, and R. A. Barrio, Phys. Rev. E **60**, 4588 (1999).
 - [15] C. Varea, J. L. Aragón, and R. A. Barrio, Phys. Rev. E **56**, 1250 (1997).
 - [16] B. Hasslacher, R. Kapral, and A. Lawniczak, Chaos **3**, 7 (1993).
 - [17] J. L. Aragon, M. Torres, D. Gil, R. A. Barrio, and P. K. Maini, Phys. Rev. E **65**, 051913 (2002).
 - [18] T. Leppänen, M. Karttunen, K. Kaski, R. A. Barrio, and L. Zhang, Physica D **168-169**, 35 (2002).
 - [19] S. L. Judd and M. Silber, Physica D **136**, 45 (2000).
 - [20] I. Lengyel and I. R. Epstein, Proc. Nat. Acad. Sci. **89**, 3977 (1992).
 - [21] J. Hoshen and R. Kopelman, Phys. Rev. B **14**, 3438 (1976).
 - [22] G. I. Barenblatt, *Dimensional Analysis* (Gordon and Breach Science Publishers, New York, 1987).
 - [23] M. Karttunen, N. Provatas, T. Ala-Nissila, and M. Grant, J. Stat. Phys. **90**, 1401 (1998).
 - [24] L. Yang, M. Dolnik, A. M. Zhabotinsky, and I.R. Epstein, Phys. Rev. Lett. **88**, 208303 (2002).
 - [25] M. Karttunen, M. Haataja, K. R. Elder, and M. Grant, Phys. Rev. Lett. **83**, 3518 (1999).
 - [26] N. W. Ashcroft and N. D. Mermin, *Solid State Physics* (Saunders College Publishing, Fort Worth, 1976).
 - [27] H.S.M. Coxeter *Regular Polytopes* (Dover, New York, 1973).
 - [28] M. Torres, J.L. Aragon, P. Domínguez, and D. Gil, J. Math. Biol. **44**, 330 (2002). J.L. Aragón, A. Gómez, and M. Torres, *Eutacticity in Nature*, (to be published).
 - [29] M. Sahimi, *Applications of Percolation Theory* (Taylor & Francis Ltd, London, UK, 1994).